Letter

# Measurement of total phase fluctuation in cold-atomic quantum simulators

Taufiq Murtadho [1,*] Federica Cataldini [2] Sebastian Erne [2] Marek Gluza [1] Mohammadamin Tajik [2] Jörg Schmiedmayer [2] and Nelly H. Y. Ng [1,†]

[1]School of Physical and Mathematical Sciences, Nanyang Technological University, Singapore 639673

[2]Vienna Center for Quantum Science and Technology, Atominstitut, TU Wien, Stadionallee 2, 1020 Vienna, Austria

(Received 18 October 2024; accepted 28 February 2025; published 7 May 2025)

Studying the dynamics of quantum many-body systems is often constrained by the limitations in probing relevant observables, especially in continuous systems. A powerful method to gain information about such systems is the reconstruction of local currents from the continuity equation. We show that this approach can be used to extract the total phase fluctuation of adjacent Bose gases. We validate our technique numerically and demonstrate its effectiveness by analyzing data from selected experiments simulating 1D quantum field theories through the phase difference of two parallel 1D Bose gases. This analysis reveals the previously hidden sector of the sum mode of the phase, which is important for studying long-time thermalization and out-of-equilibrium dynamics of the system. Our method is general and can be applied to other cold atom systems with spatial phase gradients, thereby expanding the scope and capabilities of cold-atomic quantum simulators.

DOI: 10.1103/PhysRevResearch.7.L022031

*Introduction.* Quantum many-body systems are quantum simulators for a large variety of phenomena in and out of equilibrium [1–3]. In particular, ultracold atoms have emerged as powerful and versatile platforms for simulating discrete [4–6] and continuous variable (i.e., quantum field) [7] systems. Yet, there remain several obstacles preventing them from unleashing their full potential. One major bottleneck is the limited available methods for reading out information from the simulators [8,9], especially for quantum field simulators [10,11].

A notably powerful example thereof is one-dimensional (1D) superfluids, which have enabled the observation of prethermalization [12], light cone dynamics [13,14], generalized statistical ensembles [15], recurrences [16], the area law of mutual information [17], Landauer's principle [18], and the strongly correlated sine-Gordon field theory through the evaluation of many-body correlations [19,20]. All of these studies are based on extracting local relative phases between two parallel 1D superfluids by measuring interference patterns after free expansion [21–23]. In the case of Gaussian states, its canonical conjugate—the relative density fluctuation—can also be reconstructed utilizing a coherent Tomonaga-Luttinger liquid evolution [10,24]. However, the relative phase and relative density fluctuations are still only two out of the four fields characterizing the system. Knowledge about the dynamics in the total sector, i.e., the sum rather than the difference of fluctuations in both density and phases, becomes important when studying long-time thermalization behavior [25–28] or testing the validity of the quantum field simulators [12–19], which rely on a separation between the difference and the total sectors [29]. A direct reconstruction of the single shot total phase profiles has so far been missing in experiments.

In this Letter, we present a general method for reconstructing the potential of irrotational flows from the continuity equation and apply it to extract the full counting statistics of the total phase field. We demonstrate the validity and applicability of our method by extracting the total phase of a pair of parallel 1D superfluids from the measurement of density ripples (matter wave speckles) [30–34] after free expansion. Nonetheless, our method is general and can be applied to other cold atom systems with spatial phase gradients, thereby expanding the scope and capabilities of cold-atomic quantum simulators.

*Extracting total phase from total density current.* We first consider two adjacent quasicondensates ($a = 1, 2$) each described by a bosonic field operator $\hat{\psi}_a(\mathbf{r}) = e^{i\hat{\phi}_a(\mathbf{r})}\sqrt{\hat{n}_a(\mathbf{r})}$ where $\hat{\phi}_a(\mathbf{r})$ and $\hat{n}_a(\mathbf{r})$ are the phase and density fields, respectively. We show how to extract the statistics of the total phase field

$$\hat{\phi}_+(\mathbf{r}) \coloneqq \hat{\phi}_1(\mathbf{r}) + \hat{\phi}_2(\mathbf{r}) \tag{1}$$

at time $\tau = 0$ from single-shot measurements of total density $\hat{n}_+(\mathbf{r}, \tau) \coloneqq \hat{n}_1(\mathbf{r}, \tau) + \hat{n}_2(\mathbf{r}, \tau)$ following a unitary evolution $\tau > 0$.

Our method is motivated by experiments which give access to $\hat{n}_+(\mathbf{r}, \tau)$ after time of flight, but can be generalized to arbitrary charges and irrotational currents $\hat{\mathbf{j}}_a(\mathbf{r}, \tau)$ satisfying a continuity equation $\partial_t \hat{n}_a(\mathbf{r}, \tau) + \nabla \cdot \hat{\mathbf{j}}_a(\mathbf{r}, \tau) = 0$. Such irrotational flows can be expressed as the gradient of a potential, e.g., in our case $\hat{\mathbf{j}}_a(\mathbf{r}, \tau) \approx (\hbar/m) n_a(\mathbf{r}, \tau) \nabla \hat{\phi}_a(\mathbf{r}, \tau)$ valid up to first order in the fields, with $m$ being the atomic mass, and

*Contact author: fiqmurtadho@gmail.com

†Contact author: nelly.ng@ntu.edu.sg

$n_a(\mathbf{r},\tau) = \langle \hat{n}_a(\mathbf{r},\tau)\rangle$ is the mean density. We consider short enough time scales so that the continuity equation for $\hat{n}_+(\mathbf{r},\tau)$ can be linearized as

$$\hat{n}_+(\mathbf{r},\tau) \approx n_0(\mathbf{r}) + \delta\hat{n}_+(\mathbf{r}) - \tau\nabla\cdot\hat{\mathbf{j}}_+(\mathbf{r}), \tag{2}$$

where $n_0(\mathbf{r}) \coloneqq n_1(\mathbf{r},0) + n_2(\mathbf{r},0)$ is the initial total mean density, $\delta\hat{n}_+(\mathbf{r}) \coloneqq \delta\hat{n}_1(\mathbf{r},0) + \delta\hat{n}_2(\mathbf{r},0)$ is the initial total density fluctuation, and $\hat{\mathbf{j}}_+(\mathbf{r}) \coloneqq \hat{\mathbf{j}}_1(\mathbf{r},0) + \hat{\mathbf{j}}_2(\mathbf{r},0)$ is the initial total current. In the quasicondensate regime, density fluctuations are suppressed $\delta n_+(\mathbf{r}) \ll n_0(\mathbf{r})$, and therefore can be ignored [35]. In the case of equal mean densities $n_1(\mathbf{r},0) = n_2(\mathbf{r},0) = n_0(\mathbf{r})/2$, the total current is proportional to the gradient of total phase $\nabla\hat{\phi}_+(\mathbf{r})$, which is the observable we want to measure.

We then find an operator-valued Poisson's equation (see Appendix A for derivation and generalization)

$$\ell_\tau^2\nabla^2\hat{\phi}_+(\mathbf{r}) \approx \left(1 - \frac{\hat{n}_+(\mathbf{r},\tau)}{n_0(\mathbf{r})}\right), \tag{3}$$

where $\ell_\tau = \sqrt{\hbar\tau/(2m)}$ is the dynamical length which sets the scale for spatial gradients, implying that Eq. (3) can only resolve $\hat{\phi}_+(z)$ fluctuations with length scale $\ell_\tau$. In deriving Eq. (3), we ignored the effect of inhomogeneity to the divergence of current $\nabla\cdot\hat{\mathbf{j}}_+(\mathbf{r})$, valid for sufficiently smooth $n_0(\mathbf{r})$ over a distance $\ell_\tau$.

By measuring $\hat{n}_+(\mathbf{r},\tau)$, we obtain a scalar density distribution $n_+(\mathbf{r},\tau)$ which is related to the single-shot total phase profile $\phi_+(\mathbf{r})$ through Eq. (3). The mean density $n_0(\mathbf{r})$ solves the Gross-Pitaevskii equation for a given trapping potential [10]. Thus, extracting $\phi_+(\mathbf{r})$ corresponds to solving the Poisson's Eq. (3), whose solution is unique up to a constant. Our argument is general and can be extended to an arbitrary number of quasicondensates (Appendix A).

*Total phase extraction in parallel 1D superfluids.* We now apply our method to a quantum field simulator consisting of two parallel 1D quasicondensates extended along the $z$ direction [Fig. 1(a)], each with length $L$ and mean density $n_0(z)/2$. Excitations in the system can be described by the total (+) and relative (−) phase and density fluctuations $\hat{\phi}_\pm(z) = \hat{\phi}_1(z) \pm \hat{\phi}_2(z)$ and $\delta\hat{n}_\pm(z) = \delta\hat{n}_1(z) \pm \delta\hat{n}_2(z)$, which evolve according to the system's low-energy Hamiltonian [24,29]. Here, we make no assumption about the system's evolution in the trap and focus only on the measurement process.

In typical experiments, the two gases are imaged after time of flight (TOF), i.e., after they are released from the trap and allowed to expand and interfere. The statistics of the relative phase $\hat{\phi}_-(z)$ is subsequently extracted from density interference patterns [37,38]. Our goal is to additionally read out the total phase $\hat{\phi}_+(z)$ up to a constant from the projected density data after TOF. Measuring both phases is relevant for probing interaction between the difference and the sum sectors, and for full tomography of the system.

Let $\Psi_{1,2}(r,z,\tau)$ be the atomic fields after expansion time $\tau$, including both radial $r = (x,y)$ and longitudinal $(z)$ components. We assume the *in situ* ($\tau = 0$) radial components to be Gaussian of width $\sigma_0 = \sqrt{\hbar/(m\omega_\perp)} < d$ localized around $(x,y) = (\pm d/2, 0)$ with $\omega_\perp$ being the transverse trapping frequency [39], and $d$ being the initial distance between the condensates. The *in situ* longitudinal components are modeled as stochastic scalar fields in the classical field approximation [40,41] with each sample interpreted as a single experimental realization. We focus on 1D density ripples after interference

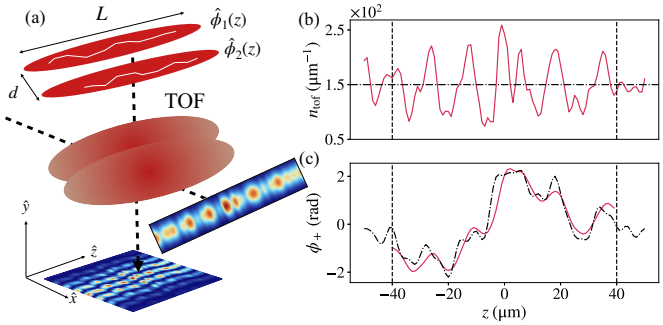


FIG. 1. Total phase profile extraction in 1D. (a) Parallel 1D quasicondensates undergoing free expansion in time of flight (TOF) and then imaged vertically (i.e., along the $y$ direction) or transversally (i.e., along the $x$ direction). Density ripple (b) is obtained after integrating the image perpendicular to the $z$ direction. The dashed-dotted line is the mean *in situ* density, which for simplicity assumed to be uniform $n_0 = 150\ \mu\text{m}^{-1}$ in the simulations, but our method is also applicable to a smooth nonuniform mean density such as that of a harmonic trap (see the Supplemental Material [36]). (c) The extracted total phase $\phi_+^{(\text{out})}(z)$ (solid red) compared with the input $\phi_+^{(\text{in})}(z)$ (black dashed dotted). We only implement the extraction in the bulk (between the dashed lines) $z \in [-\mathcal{L}/2, \mathcal{L}/2]$ with $\mathcal{L} < L$ and $L$ is the initial length of the gas (before TOF). For our simulations, we use $L = 100\ \mu\text{m}$ and $\mathcal{L} = 80\ \mu\text{m}$ with 1 $\mu$m lattice spacing. Other parameters are $d = 2\ \mu\text{m}$, $\omega_\perp = 2\pi \times 1.4$ kHz, $a_s = 5.2$ nm, and $m$ is the mass of $^{87}$Rb. The statistics of the field $\hat{\phi}_+(z)$ is reconstructed by measuring over many shots.

$$n_{\rm tof}(z,\tau) \coloneqq \int |\Psi_1(r,z,\tau) + \Psi_2(r,z,\tau)|^2\, dr, \tag{4}$$

routinely measured in experiments by transversal imaging or by integrating interference patterns obtained from vertical imaging [Fig. 1(a)]. The evolved fields $\Psi_{1,2}(r,z,\tau)$ are related to the *in situ* fields through TOF dynamics, which we model as ballistic expansion, i.e., $\Psi_{1,2}(r,z,\tau) = \int d^3\mathbf{r}' G^{(3)}(\mathbf{r}-\mathbf{r}',\tau)\Psi_{1,2}(r',z',0)$ with $G(\xi,\tau) = \sqrt{m/(2\pi i\hbar\tau)}\exp[-m\xi^2/(2i\hbar\tau)]$ being the free particle propagator. This is justified due to the fast expansion of the gas in the radial direction which causes interaction to quickly decay [22,23,32].

We show in Appendix B that the interference contribution $\int \text{Re}(\Psi_1^*\Psi_2)dr$ to Eq. (4) is strongly suppressed by a factor $e^{-m\omega_\perp d^2/(4\hbar)} \sim 10^{-6}$ for typical experimental parameters compared to the sum of individual densities $\int(|\Psi_1|^2 + |\Psi_2|^2)dr = n_+(z,\tau)$, and hence can be ignored. The dynamics of $n_+(z,\tau)$ encodes $\phi_+(z)$ information via the mass current $j_+(z) = (\hbar/2m)\partial_z(n_0(z)\phi_+(z))$, i.e., in positions where $\partial_z j_+ > 0$ ($\partial_z j_+ < 0$), there is more mass going out (in) than going in (out) of an infinitesimal element, leading to depletion (accumulation) of local density during the expansion [Fig. 1(b)]. To extract $\phi_+(z)$, we solve the 1D version of Eq. (3) with the normalized density ripples as the source term.

*Extraction performance.* We evaluate the extraction performance through numerical simulation consisting of three

stages: (i) sampling *in situ* phase and density fluctuations, (ii) simulating TOF dynamics which encodes the sampled phases into density distributions, and (iii) reconstructing the encoded total phases from density ripples.

We sample the *in situ* fluctuations from Bogoliubov modes [16,42] assuming a thermal state of decoupled uniform gases

$$\phi_+^{(\mathrm{in})}(z) = \frac{1}{\sqrt{n_0 L}} \sum_{k\neq 0} \sqrt{\frac{\varepsilon_k}{E_k}} b_k e^{ikz} + \mathrm{H.c.}, \tag{5}$$

where $\varepsilon_k = \sqrt{E_k(E_k + gn_0)}$ is the Bogoliubov spectrum, $E_k = (\hbar k)^2/2m$ is the free dispersion, $g \approx 2\hbar\omega_\perp a_s$ is the 1D interaction strength, and $a_s$ is the scattering length [43]. The occupation $b_k$ is sampled from a Bose-Einstein distribution with temperature $T_+$. The summation is taken over $k = 2\pi p/L$ with $p$ nonzero integers up to a cutoff $p_{\max}$. Similar expansion also holds for the other fields, see the Supplemental Material [36].

For each sample, we compute the density ripple $n_{\mathrm{tof}}(z,\tau)$ with Eq. (4). We then extract the total phase in the bulk by solving Eq. (3) using the finite difference method. Arbitrary boundary conditions in the region of interest are handled by smoothly extrapolating the data and imposing Dirichlet boundary conditions in the extended domain. The global phase is fixed to zero by $\int \phi_+(z)\, dz = 0$. We repeat the procedure for $10^3$ shots. Single-shot examples are shown in Fig. 1(c) and in the Supplemental Material [36].

Here, we compare the correlation functions of the input samples and the reconstructed profiles. We first study the reconstruction of the vertex correlation function [24]

$$C_+(z,z') \coloneqq \mathrm{Re}[\langle e^{i(\phi_+(z)-\phi_+(z'))}\rangle], \tag{6}$$

where $\langle\ \rangle$ denotes the average over realizations. The associated correlation function in the relative sector has been used in many 1D gases experiments [13,16]. It is also recently pointed out that $C_+(z,z')$ is a useful probe to study postquench relaxation of unequal pair of Luttinger liquids [44]. Here, we instead focus on thermal equilibrium. For a thermal state of uniform decoupled gases with $L\to\infty$, the correlation decays exponentially with distance $\Delta z \coloneqq |z-z'|$, i.e., $C_+(z,z') \sim \exp(-\Delta z/\lambda_{T_+})$ for thermal coherence length $\lambda_{T_+} = \hbar^2 n_0/(2mk_B T_+)$. Hence, the decay of $C_+(z,z')$ provides an alternative method to density ripple thermometry [32,33,36,45].

The reconstructions of $C_+(z,z')$ for input samples with $T_+ = 50$ nK are shown in Figs. 2(a) and 2(b) for two different expansion times $\tau = 11$ ms and $\tau = 16$ ms, a choice motivated by experimental examples in the next section. We find that we can reliably reconstruct $C_+(z,z')$ in both cases. In Fig. 2(a), we display a slice $C_+(z,z'=0)$ and compare the input and the reconstructed correlations. For short distances, the $\tau = 11$ ms reconstruction is more faithful due to better spatial resolution (shorter $\ell_\tau$). However, we find that the $\tau = 16$ ms reconstruction performs better in long distances. We average all $C_+(z,z')$ with fixed $\Delta z = |z-z'|$ and extract temperatures by linear fitting in log scale [Fig. 2(b)]. From the input samples, we fit a temperature $T_+ = 41$ nK $< 50$ nK due to the finite length effect [36]. Interestingly, we obtain fits closer to the true

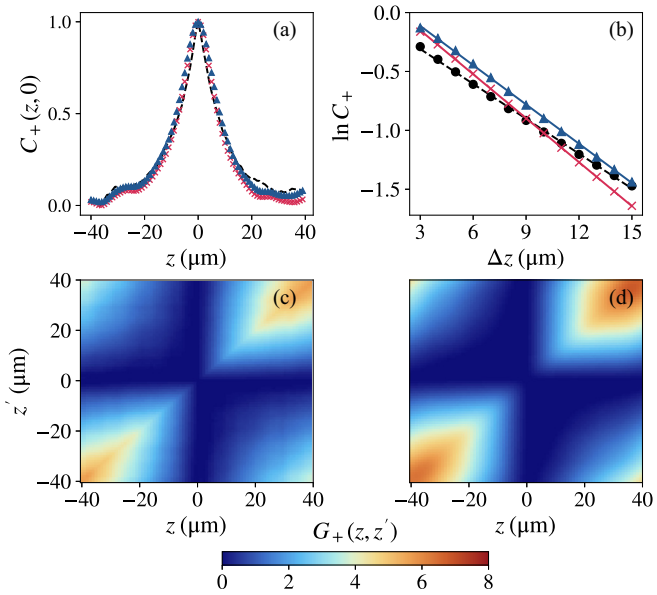


FIG. 2. Extraction performance. (a) A slice of vertex correlation function $C_+(z,z'=0)$ computed from $10^3$ input samples $\{\phi_+^{(\mathrm{in})}(z)\}$ with $T_+ = 50$ nK (black dashed line) compared to TOF reconstructions $\{\phi_+^{(\mathrm{out})}(z)\}$ with $\tau = 11$ ms (red crosses) and $\tau = 16$ ms (blue triangles). (b) Averaged $C_+(\Delta z)$ as a function of $\Delta z = |z-z'|$ in the bulk plotted in log scale. Thermal coherence lengths $\lambda_{T_+}$ and temperatures $T_+$ are extracted by linear fit. Panels (c) and (d) show the two-point correlation functions $G_+(z,z')$ computed from (c) input samples and (d) $\tau = 16$ ms TOF reconstruction. The $\tau = 11$ ms reconstruction is similar and shown in Supplemental Material [36]. The cutoff is set to $p_{\max} = 50$ and the temperature of the relative fields is fixed at $T_- = 30$ nK. Other parameters are the same as in Fig. 1.

temperature from the reconstructed profiles, i.e., $T_+ = 52$ nK ($\tau = 11$ ms) and $T_+ = 46.5$ nK ($\tau = 16$ ms). We observe the same trend for different values of the true temperature.

We also study the reconstruction of the two-point correlation function

$$G_+(z,z') \coloneqq \langle[\phi_+(z)-\phi_+(0)][\phi_+(z')-\phi_+(0)]\rangle, \tag{7}$$

which is important for quadrature tomography [10] and studying non-Gaussianity [19] in the total sector. We demonstrate in Figs. 2(c) and 2(d) that our extraction can faithfully reconstruct $G_+(z,z')$. In addition, we show in the Supplemental Material [36] that we can faithfully reconstruct the full contrast distribution function [38,42] of the total phase.

*Applications to experiments.* We next demonstrate total phase extraction by analyzing two different 1D ultracold atom experiments. In the first experiment, total phase relaxation dynamics in driven Luttinger liquids is investigated. Two parallel and independent 1D quasicondensates are prepared in a thermal state and trapped in a boxlike potential of length $L$ at $t = -t_0$, see the Supplemental Material [36] for details. For $-t_0 < t < 0$, the second phononic mode $k_2 = 2\pi/L$ is excited by modulating the box walls at the resonant frequency $\omega_2 = ck_2$, $c$ being the speed of sound. The modulation excites the total phase mode resonant to the drive, thereby imprinting a specific phase pattern to be reconstructed. At $t = 0$, we stop the driving and let the system evolve ($t > 0$). The dynamics

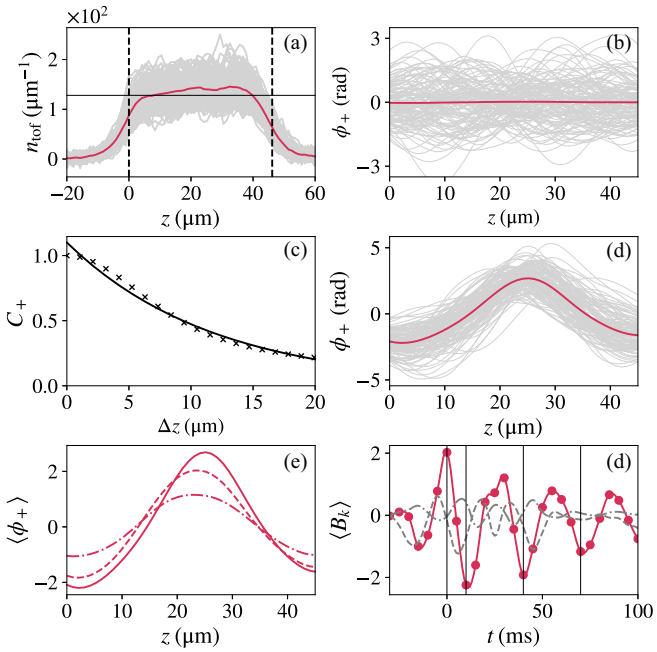


FIG. 3. Total phase dynamics after driving. (a) Density ripples $n_{\rm tof}(z)$ (gray) from thermal equilibrium state ($t = -t_0$) of a boxlike potential measured after $\tau = 11.2$ ms TOF. Mean density $n_0(z)$ (red) is estimated from the ensemble average. The dashed lines indicate the (approximate) box position of length $L \approx 46(3)$ μm. The solid horizontal line is the approximate linear mean density $n_0 \approx 128(10)$ μm$^{-1}$ obtained by averaging $n_0(z)$ within the box. (b) Extracted $\phi_+(z)$ from density ripples in (a). Each gray line represents a single realization of $\phi_+(z)$ and the red line shows the mean signal $\langle\phi_+(z)\rangle$. (c) Thermal vertex correlation function $C_+(\Delta z)$ (crosses) and its exponential fit (solid line), from which we extract temperature $T_+ = 31(3)$ nK. (d) Single shots (gray) and mean (red) total phase at $t = 10$ ms after the driving is turned off. We observe clear excitation of the resonant mode ($k_2 = 2\pi/L$) in the mean signal. (e) Damped recurrence of $\langle\phi_+(z)\rangle$ at $t = 10$ ms (solid), $t = 40$ ms (dashed dotted), and $t = 70$ ms (dashed). (f) The mean occupation $\langle B_k(t)\rangle$ associated with the resonant mode $k_2$ (red circles) oscillating with period $\tau_2 = 2\pi/(ck_2) \approx 30$ ms. The vertical black lines indicate $t = 0, 10, 40, 70$ ms. The gray dashed-dotted line shows minor excitation of the off-resonant mode $k_3 = 3\pi/L$ oscillating with period $\tau_3 = 2\pi/(ck_3) \approx 20$ ms. The bias in the resonant signal and the dynamics of $k_1 = \pi/L$ (gray dashed line) are artefacts from boundary effects. The evolution is probed with a time step $\Delta t = 5$ ms and ∼130 shots at each time step. The driving frequency is $\omega_2 = 2\pi \times 36$ Hz and speed of sound is $c \approx 1.8$ μm/ms for each quasicondensate.

of the system is probed by performing density measurements $n_{\rm tof}(z, t)$ after $\tau = 11.2$ ms TOF, at different evolution times $t$ and repeated over ∼130 experimental shots for each $t$.

The density ripples in thermal equilibrium ($t = -t_0$) are shown in Fig. 3(a), from which thermal fluctuation of the total phase is reconstructed in Fig. 3(b). Exponential fit to the vertex correlation function $C_+(\Delta z)$ shown in Fig. 3(c) yields thermal coherence length $\lambda_{T_+} = 11.8(3)$ μm equivalent to temperature $T_+ = 31(3)$ nK, which agrees with the result obtained using density ripple thermometry [36].

After the system is let to naturally evolve ($t > 0$), we expect $\phi_+(z)$ to be the sum of two contributions, (i) excitation due to the modulation $\phi_+^{(\rm mod)}(z)$ and (ii) thermal fluctuation $\delta\phi_+^{(\rm th)}(z)$. On average, thermal contribution vanishes so we expect the first moment to contain only the modulation signal $\langle\phi_+(z)\rangle \approx \langle\phi_+^{(\rm mod)}(z)\rangle$. In Fig. 3(d), we show both the fluctuations and the mean signal at $t = 10$ ms. As we expect, the mean signal displays a clear excitation of the resonant mode. Furthermore, in Fig. 3(e), we observe recurrences of the signal with $\mathcal{T}_2 \approx 30$ ms period as expected from Luttinger liquid theory. The observed amplitude damping can be due to corrections to the effective Luttinger liquid model [46] or due to other sources of dissipation. We analyze the mean extracted phase $\langle\phi_+(z, t)\rangle$ by expanding it in cosine series $\langle\phi_+(z, t)\rangle = \sum_k \langle B_k(t)\rangle \cos(kz)$ with $k = p\pi/L$ and $p$ positive integers. In Fig. 3(f), we show mean occupation $\langle B_k(t)\rangle$ for the first three modes, illustrating a clear resonance and oscillation of the second mode. We also observe a minor off-resonant excitation with period $\mathcal{T}_3 \approx 20$ ms associated with the third mode $k_3 = 3\pi/L$. The oscillation observed in $k_1 = \pi/L$ mode and the bias in the resonant signals are artifacts from boundary effects.

In the second example, we probe the dynamics of the total phase after a quench from a strongly correlated state to a free system (Gaussification experiment [20,36,47]). The initial state is prepared in thermal equilibrium of a double-well potential with finite tunnel coupling, and set in a regime where the relative phase follows non-Gaussian correlations, that is the state of the simulated sine-Gordon field is strongly correlated [19]. The relative phase then evolves to an uncorrelated Gaussian state after quenching the tunnel coupling to zero by ramping up the double well barrier. In the low-energy approximation, the total sector is expected to be decoupled from the relative sector and described by a Luttinger liquid [29].

To investigate the dynamics of the total phase after the quench, we first obtain density ripples data by integrating the interference pictures along the transverse direction [Figs. 4(a) and 4(b)]. Then, using our method, we extract $\phi_+(z)$ for each shot. We calculate the vertex correlation function $C_+(\Delta z, t)$ as a function of evolution time $t$ and find it to be approximately static [Fig. 4(c)] with coherence length $\lambda_+ \approx 11-13$ μm [Fig. 4(d)]. This coherence length is approximately the same as the thermal coherence length of the relative phase [20], confirming that the two sectors are initially in thermal equilibrium. Our analysis suggests a separation between the sum and the difference sectors as predicted by the low-energy approximation. However, definitively establishing the separation between the two sectors requires a more detailed analysis involving higher-order correlations, which is a subject for future work.

*Summary and outlook.* We presented the reconstruction of total phase full counting statistics for adjacent quasicondensates by inverting a continuity equation. Our approach reveals information about the sum modes in parallel 1D superfluids, allowing one to compute all phase correlation functions of the system if combined with the standard relative phase extraction through interference. We validated our method numerically and experimentally by reconstructing thermal correlation functions and observing the dynamics of the total phase after driving and quenching.

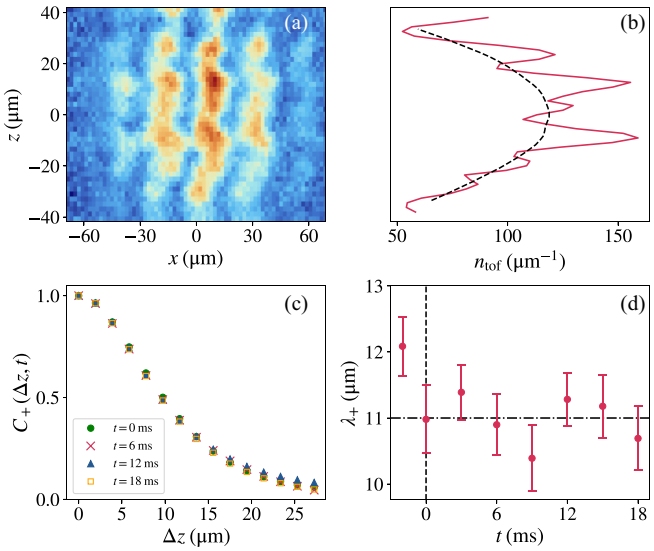


FIG. 4. Total phase dynamics after a quench. (a) An example of interference pictures used to probe the relative phase. (b) Density ripple is obtained by integrating the picture in the transverse $x$ direction. The postquench evolution is probed every $\Delta t = 3$ ms by vertically imaging the atoms after $\tau = 15.6$ ms TOF and repeated $\sim$500 times for each evolution time $t$. The mean density is estimated by ensemble averaging (dashed line). (c) The vertex correlation function $C_+(\Delta z, t)$ calculated from the data is approximately static. (d) The fitted coherence length $\lambda_+(t)$ stays approximately constant within the error bars. The $t = 0$ ms (dashed line) marks the time when the quench is completed. The dashed-dotted line is the thermal coherence length of the relative phase [20]. Our analysis suggests that in contrast to the relative phase, the total phase stays thermal and at constant temperature throughout the evolution.

In this work, we focus on cases where it is sufficient to linearize the continuity equation and solve the resulting Poisson's equation. However, in cases where linearization might fail, such as for long expansion times or strong final-state interaction [48,49], one can instead numerically invert the continuity equation, for example, by using physics-informed neural networks [50].

Our extraction enables tackling relaxation dynamics [25–28], testing the applicability limits of low-energy effective models [51–53], and performing full quantum field tomography [10,54]. Our approach is general and can be applied to other systems with spatial phase gradients such as $N$ quasicondensates [55], 2D Bosonic gases [56–58], and ultracold atoms in optical lattices [9,11,59,60]. Thus, our work expands the scope and capabilities of quantum simulation for studying quantum matter in and out of equilibrium.

*Acknowledgments.* We thank Thomas Schweigler for sharing the original data of the Gaussification experiment [20]. T.M., M.G., and N.H.Y.N. were supported through the start-up grant of the Nanyang Assistant Professorship of Nanyang Technological University, Singapore, which was awarded to N.H.Y.N. Additionally, M.G. has been supported by the Presidential Postdoctoral Fellowship of the Nanyang Technological University. The experiments in Vienna are supported by the Austrian Science Fund (FWF) (Grant No. I6276, QuFT-Lab) and the ERC-AdG: Emergence in Quantum Physics (EmQ).

## APPENDIX A: EXTENSION TO $N$ QUASICONDENSATES AND TO UNEQUAL MEAN DENSITIES

Consider $N$ quasicondensates with the total phase defined as $\hat{\phi}_+(\mathbf{r}) \coloneqq \sum_{a=1}^{N} \phi_a(\mathbf{r})$ and similarly the total density is $\hat{n}_+(\mathbf{r}, \tau) \coloneqq \sum_{a=1}^{N} \hat{n}_a(\mathbf{r})$. We first assume identical mean densities for each quasicondensate, i.e., $n_a(\mathbf{r}) \coloneqq \langle \hat{n}_a(\mathbf{r}) \rangle = n_0(\mathbf{r})/N$. The linearized continuity equation is then written as

$$\hat{n}_+(\mathbf{r}, \tau) \approx \hat{n}_+(\mathbf{r}) - \ell_\tau^2 \nabla \cdot (n_0(\mathbf{r}) \nabla \hat{\phi}_+(\mathbf{r})), \tag{A1}$$

where $\ell_\tau \coloneqq \sqrt{\hbar\tau/(Nm)}$. The first term contains the initial density distribution $\hat{n}_+(\mathbf{r}, 0) \coloneqq \hat{n}_+(\mathbf{r})$ given by

$$\hat{n}_+(\mathbf{r}) = n_0(\mathbf{r}) + \delta\hat{n}_+(\mathbf{r}) \approx n_0(\mathbf{r}), \tag{A2}$$

where in the approximation we have ignored the initial total density fluctuation $\delta\hat{n}_+(\mathbf{r}) \coloneqq \sum_{a=1}^{N} \delta\hat{n}_a(\mathbf{r})$. Meanwhile, the second term in Eq. (A1) is

$$n_0(\mathbf{r}) \left[ \ell_\tau^2 \nabla^2 \hat{\phi}_+ + \frac{\ell_\tau \nabla n_0(\mathbf{r})}{n_0(\mathbf{r})} \cdot (\ell_\tau \nabla \hat{\phi}_+) \right] \approx n_0(\mathbf{r}) \ell_\tau^2 \nabla^2 \hat{\phi}_+, \tag{A3}$$

where we have ignored the second term in the square bracket, justified for typical smooth profiles, e.g., within the bulk of a harmonic trap [36]. Substituting Eqs. (A2) and (A3) into Eq. (A1), one can derive the Poisson's Eq. (3) in the main text for arbitrary $N$.

Next, we extend our result to nonidentical mean density for $N = 2$, i.e., $n_1(\mathbf{r}) \neq n_2(\mathbf{r})$, relevant for studying the interaction between relative and total sectors in Luttinger liquids [44,61]. In this case, the linearized continuity equation is

$$\hat{n}_+(\mathbf{r}, \tau) \approx n_0(\mathbf{r}) - \frac{\hbar\tau}{m} \sum_{a=1}^{2} \nabla \cdot (n_a(\mathbf{r}) \nabla \hat{\phi}_a(\mathbf{r})). \tag{A4}$$

We perform a change of basis by expressing $\hat{\phi}_{1,2}(\mathbf{r})$ in terms of $\hat{\phi}_\pm(\mathbf{r})$ and then solve for $\hat{\phi}_+(\mathbf{r})$. The result is

$$\ell_\tau^2 \nabla^2 \hat{\phi}_+(\mathbf{r}) \approx \left(1 - \frac{\hat{n}_+(\mathbf{r}, \tau)}{n_0(\mathbf{r})}\right) - \frac{\Delta n(\mathbf{r})}{n_0(\mathbf{r})} \ell_\tau^2 \nabla^2 \hat{\phi}_-(\mathbf{r}), \tag{A5}$$

where $n_0(\mathbf{r}) = n_1(\mathbf{r}) + n_2(\mathbf{r})$ and $\Delta n(\mathbf{r}) = n_1(\mathbf{r}) - n_2(\mathbf{r})$. In other words, the source term in the Poisson's equation acquires a correction proportional to the density imbalance and the Laplacian of the relative phase. The latter can be extracted from the interference pictures.

## APPENDIX B: INDEPENDENCE OF DENSITY RIPPLES FROM INTERFERENCE

Here, we prove that one can ignore interference terms when analyzing density ripples after free expansion. We start from the expression of the initial fields

$$\Psi_{1,2}(\mathbf{r}, 0) = \frac{1}{\sqrt{\pi\sigma_0^2}} \exp\left[ -\frac{(x \pm d/2)^2 + y^2}{2\sigma_0^2} \right] \psi_{1,2}(z, 0), \tag{B1}$$

where $\sigma_0 = \sqrt{\hbar/(m\omega_\perp)}$ is the initial Gaussian width in the transverse direction, $d$ is the initial separation of the two

gases, and $\psi_{1,2}(z,0) = e^{i\phi_{1,2}(z)}\sqrt{n_{1,2}(z)+\delta n_{1,2}(z)}$ are the initial longitudinal components of the fields. Convolving these fields with respect to the free particle Green's function $G(\mathbf{r}-\mathbf{r}',\tau)$, we obtain the evolved fields after some expansion time $\tau$,

$$\Psi_{1,2}(\mathbf{r},\tau) = \frac{1}{\sqrt{\pi\sigma_0^2(1+i\omega_\perp\tau)^2}}\exp\left(-\frac{(x\pm d/2)^2+y^2}{2\sigma_0^2(1+i\omega_\perp\tau)}\right) \times \exp\left(\frac{im[(x\pm d/2)^2+y^2]}{2\hbar\tau}\right)\psi_{1,2}(z,\tau), \tag{B2}$$

where $\psi_{1,2}(z,\tau) = \int G(z-z',\tau)\psi_{1,2}(z',0)\,dz'$ are the evolved longitudinal fields.

We are interested in density ripples after interference [Eq. (4) in the main text]:

$$n_{\rm tof}(z,\tau) = \int |\Psi_1(\mathbf{r},\tau)+\Psi_2(\mathbf{r},\tau)|^2\,dx\,dy \approx \int Ae^{-\frac{x^2}{\sigma_\tau^2}}|e^{\frac{iqx}{2}}\psi_1(z,\tau)+e^{-\frac{iqx}{2}}\psi_2(z,\tau)|^2dx, \tag{B3}$$

with $A$ being normalization constant, $\sigma_\tau = \sigma_0\sqrt{1+\omega_\perp^2\tau^2}$ being the expanded width, and $q = md/(\hbar\tau)$ being the inverse fringe spacing. To derive the second line, we have used the approximation $d \ll \sigma_\tau$ necessary for the two fields to significantly overlap. Performing the integration with respect to $x$ yields

$$n_{\rm tof}(z,\tau) \approx |\psi_1(z,\tau)|^2+|\psi_2(z,\tau)|^2 + 2e^{-(q\sigma_\tau/2)^2}{\rm Re}[\psi_1^*(z,\tau)\psi_2(z,\tau)]. \tag{B4}$$

The first line in Eq. (B4) is the contribution from individual densities while the second line is due to interference. For $\omega_\perp\tau \gg 1$, the exponent in the interference term is approximately

$$\left(\frac{q\sigma_\tau}{2}\right)^2 \approx \frac{m\omega_\perp d^2}{4\hbar} \approx 12, \tag{B5}$$

where we have plugged in typical experimental parameters $\omega_\perp = 2\pi\times 1.4$ kHz, $d = 2$ μm, and $m$ is the mass of $^{87}$Rb. This implies that the interference term is strongly suppressed by a factor of $e^{-12} \sim 10^{-6}$ compared to the individual density contribution, and hence can be ignored.


[1] I. M. Georgescu, S. Ashhab, and F. Nori, Quantum simulation, Rev. Mod. Phys. **86**, 153 (2014).

[2] E. Altman, K. R. Brown, G. Carleo, L. D. Carr, E. Demler, C. Chin, B. DeMarco, S. E. Economou, M. A. Eriksson, K.-M. C. Fu, M. Greiner, K. R. Hazzard, R. G. Hulet, A. J. Kollár, B. L. Lev, M. D. Lukin, R. Ma, X. Mi, S. Misra, C. Monroe *et al.*, Quantum simulators: Architectures and opportunities, PRX Quantum **2**, 017003 (2021).

[3] A. J. Daley, Twenty-five years of analogue quantum simulation, Nat. Rev. Phys. **5**, 702 (2023).

[4] I. Bloch, J. Dalibard, and S. Nascimbene, Quantum simulations with ultracold quantum gases, Nat. Phys. **8**, 267 (2012).

[5] C. Gross and I. Bloch, Quantum simulations with ultracold atoms in optical lattices, Science **357**, 995 (2017).

[6] C. Viermann, M. Sparn, N. Liebster, M. Hans, E. Kath, Á. Parra-López, M. Tolosa-Simeón, N. Sánchez-Kuntz, T. Haas, H. Strobel *et al.*, Quantum field simulator for dynamics in curved spacetime, Nature (London) **611**, 260 (2022).

[7] T. Langen, R. Geiger, and J. Schmiedmayer, Ultracold atoms out of equilibrium, Annu. Rev. Condens. Matter Phys. **6**, 201 (2015).

[8] T. Barthel and J. Lu, Fundamental limitations for measurements in quantum many-body systems, Phys. Rev. Lett. **121**, 080406 (2018).

[9] A. Impertro, S. Karch, J. F. Wienand, S. J. Huh, C. Schweizer, I. Bloch, and M. Aidelsburger, Local readout and control of current and kinetic energy operators in optical lattices, Phys. Rev. Lett. **133**, 063401 (2024).

[10] M. Gluza, T. Schweigler, B. Rauer, C. Krumnow, J. Schmiedmayer, and J. Eisert, Quantum read-out for cold atomic quantum simulators, Commun. Phys. **3**, 12 (2020).

[11] E. Wybo, A. Bastianello, M. Aidelsburger, I. Bloch, and M. Knap, Preparing and analyzing solitons in the sine-Gordon model with quantum gas microscopes, PRX Quantum **4**, 030308 (2023).

[12] M. Gring, M. Kuhnert, T. Langen, T. Kitagawa, B. Rauer, M. Schreitl, I. Mazets, D. A. Smith, E. Demler, and J. Schmiedmayer, Relaxation and prethermalization in an isolated quantum system, Science **337**, 1318 (2012).

[13] T. Langen, R. Geiger, M. Kuhnert, B. Rauer, and J. Schmiedmayer, Local emergence of thermal correlations in an isolated quantum many-body system, Nat. Phys. **9**, 640 (2013).

[14] M. Tajik, M. Gluza, N. Sebe, P. Schüttelkopf, F. Cataldini, J. Sabino, F. Møller, S.-C. Ji, S. Erne, G. Guarnieri *et al.*, Experimental observation of curved light-cones in a quantum field simulator, Proc. Natl. Acad. Sci. USA **120**, e2301287120 (2023).

[15] T. Langen, S. Erne, R. Geiger, B. Rauer, T. Schweigler, M. Kuhnert, W. Rohringer, I. E. Mazets, T. Gasenzer, and J. Schmiedmayer, Experimental observation of a generalized Gibbs ensemble, Science **348**, 207 (2015).

[16] B. Rauer, S. Erne, T. Schweigler, F. Cataldini, M. Tajik, and J. Schmiedmayer, Recurrences in an isolated quantum many-body system, Science **360**, 307 (2018).

[17] M. Tajik, I. Kukuljan, S. Sotiriadis, B. Rauer, T. Schweigler, F. Cataldini, J. Sabino, F. Møller, P. Schüttelkopf, S.-C. Ji *et al.*, Verification of the area law of mutual information in a quantum field simulator, Nat. Phys. **19**, 1022 (2023).

[18] S. Aimet, M. Tajik, G. Tournaire, P. Schüttelkopf, J. Sabino, S. Sotiriadis, G. Guarnieri, J. Schmiedmayer, and J. Eisert, Experimentally probing Landauer's principle in the quantum many-body regime, arXiv:2407.21690.

[19] T. Schweigler, V. Kasper, S. Erne, I. Mazets, B. Rauer, F. Cataldini, T. Langen, T. Gasenzer, J. Berges, and J. Schmiedmayer, Experimental characterization of a quantum many-body system via higher-order correlations, Nature (London) **545**, 323 (2017).

[20] T. Schweigler, M. Gluza, M. Tajik, S. Sotiriadis, F. Cataldini, S.-C. Ji, F. S. Møller, J. Sabino, B. Rauer, J. Eisert *et al.*, Decay and recurrence of non-Gaussian correlations in a quantum many-body system, Nat. Phys. **17**, 559 (2021).

[21] D. A. Smith, S. Aigner, S. Hofferberth, M. Gring, M. Andersson, S. Wildermuth, P. Krüger, S. Schneider, T. Schumm, and J. Schmiedmayer, Absorption imaging of ultracold atoms on atom chips, Opt. Express **19**, 8471 (2011).

[22] Y. D. van Nieuwkerk, J. Schmiedmayer, and F. Essler, Projective phase measurements in one-dimensional bose gases, SciPost Phys. **5**, 046 (2018).

[23] T. Murtadho, M. Gluza, K. Z. Arifa, S. Erne, J. Schmiedmayer, and N. H. Y. Ng, Systematic analysis of relative phase extraction in one-dimensional Bose gases interferometry, SciPost Phys. **18**, 065 (2025).

[24] T. Giamarchi, *Quantum Physics in One Dimension* (Clarendon Press, Oxford, 2003), Vol. 121.

[25] A. A. Burkov, M. D. Lukin, and E. Demler, Decoherence dynamics in low-dimensional cold atom interferometers, Phys. Rev. Lett. **98**, 200404 (2007).

[26] I. Mazets and J. Schmiedmayer, Dephasing in two decoupled one-dimensional Bose-Einstein condensates and the subexponential decay of the interwell coherence, Eur. Phys. J. B **68**, 335 (2009).

[27] S. Huber, M. Buchhold, J. Schmiedmayer, and S. Diehl, Thermalization dynamics of two correlated bosonic quantum wires after a split, Phys. Rev. A **97**, 043611 (2018).

[28] H.-P. Stimming, N. J. Mauser, J. Schmiedmayer, and I. E. Mazets, Dephasing in coherently split quasicondensates, Phys. Rev. A **83**, 023618 (2011).

[29] V. Gritsev, A. Polkovnikov, and E. Demler, Linear response theory for a pair of coupled one-dimensional condensates of interacting atoms, Phys. Rev. B **75**, 174511 (2007).

[30] S. Dettmer, D. Hellweg, P. Ryytty, J. J. Arlt, W. Ertmer, K. Sengstock, D. S. Petrov, G. V. Shlyapnikov, H. Kreutzmann, L. Santos, and M. Lewenstein, Observation of phase fluctuations in elongated Bose-Einstein condensates, Phys. Rev. Lett. **87**, 160406 (2001).

[31] D. Hellweg, S. Dettmer, P. Ryytty, J. Arlt, W. Ertmer, K. Sengstock, D. Petrov, G. Shlyapnikov, H. Kreutzmann, L. Santos *et al.*, Phase fluctuations in Bose-Einstein condensates, Appl. Phys. B **73**, 781 (2001).

[32] A. Imambekov, I. E. Mazets, D. S. Petrov, V. Gritsev, S. Manz, S. Hofferberth, T. Schumm, E. Demler, and J. Schmiedmayer, Density ripples in expanding low-dimensional gases as a probe of correlations, Phys. Rev. A **80**, 033604 (2009).

[33] S. Manz, R. Bücker, T. Betz, C. Koller, S. Hofferberth, I. E. Mazets, A. Imambekov, E. Demler, A. Perrin, J. Schmiedmayer, and T. Schumm, Two-point density correlations of quasicondensates in free expansion, Phys. Rev. A **81**, 031610(R) (2010).

[34] P. E. Tavares, A. R. Fritsch, G. D. Telles, M. S. Hussein, F. Impens, R. Kaiser, and V. S. Bagnato, Matter wave speckle observed in an out-of-equilibrium quantum fluid, Proc. Natl. Acad. Sci. USA **114**, 12691 (2017).

[35] D. S. Petrov, G. V. Shlyapnikov, and J. T. M. Walraven, Phase-fluctuating 3D Bose-Einstein condensates in elongated traps, Phys. Rev. Lett. **87**, 050404 (2001).

[36] See Supplemental Material at http://link.aps.org/supplemental/10.1103/PhysRevResearch.7.L022031 for details on the sampling method, experimental protocols, and extended numerical and experimental data.

[37] T. Schumm, S. Hofferberth, L. M. Andersson, S. Wildermuth, S. Groth, I. Bar-Joseph, J. Schmiedmayer, and P. Krüger, Matter-wave interferometry in a double well on an atom chip, Nat. Phys. **1**, 57 (2005).

[38] S. Hofferberth, I. Lesanovsky, T. Schumm, A. Imambekov, V. Gritsev, E. Demler, and J. Schmiedmayer, Probing quantum and thermal noise in an interacting many-body system, Nat. Phys. **4**, 489 (2008).

[39] Throughout this paper, we ignore interaction-induced broadening which introduces a density-dependent width $\sigma^2(z) = \sigma_0^2\sqrt{1 + a_s n_0(z)} \approx \sigma_0^2$.

[40] M. J. Steel, M. K. Olsen, L. I. Plimak, P. D. Drummond, S. M. Tan, M. J. Collett, D. F. Walls, and R. Graham, Dynamical quantum noise in trapped Bose-Einstein condensates, Phys. Rev. A **58**, 4824 (1998).

[41] A. Sinatra, C. Lobo, and Y. Castin, The truncated Wigner method for Bose-condensed gases: limits of validity and applications1, J. Phys. B **35**, 3599 (2002).

[42] H.-P. Stimming, N. J. Mauser, J. Schmiedmayer, and I. E. Mazets, Fluctuations and stochastic processes in one-dimensional many-body quantum systems, Phys. Rev. Lett. **105**, 015301 (2010).

[43] M. Olshanii, Atomic scattering in the presence of an external confinement and a gas of impenetrable bosons, Phys. Rev. Lett. **81**, 938 (1998).

[44] P. Ruggiero, L. Foini, and T. Giamarchi, Large-scale thermalization, prethermalization, and impact of temperature in the quench dynamics of two unequal Luttinger liquids, Phys. Rev. Res. **3**, 013048 (2021).

[45] F. Møller, T. Schweigler, M. Tajik, J. a. Sabino, F. Cataldini, S.-C. Ji, and J. Schmiedmayer, Thermometry of one-dimensional Bose gases with neural networks, Phys. Rev. A **104**, 043305 (2021).

[46] F. Cataldini, F. Møller, M. Tajik, J. A. Sabino, S.-C. Ji, I. Mazets, T. Schweigler, B. Rauer, and J. Schmiedmayer, Emergent Pauli blocking in a weakly interacting Bose gas, Phys. Rev. X **12**, 041032 (2022).

[47] M. Gluza, T. Schweigler, M. Tajik, J. Sabino, F. Cataldini, F. S. Møller, S.-C. Ji, B. Rauer, J. Schmiedmayer, J. Eisert *et al.*, Mechanisms for the emergence of Gaussian correlations, SciPost Phys. **12**, 113 (2022).

[48] J. N. Kupferschmidt and E. J. Mueller, Role of interactions in time-of-flight expansion of atomic clouds from optical lattices, Phys. Rev. A **82**, 023618 (2010).

[49] A. Burchianti, C. D'Errico, L. Marconi, F. Minardi, C. Fort, and M. Modugno, Effect of interactions in the interference pattern of Bose-Einstein condensates, Phys. Rev. A **102**, 043314 (2020).

[50] S. Cuomo, V. S. Di Cola, F. Giampaolo, G. Rozza, M. Raissi, and F. Piccialli, Scientific machine learning through

physics–informed neural networks: Where we are and what's next, J. Sci. Comput. **92**, 88 (2022).

[51] Y. D. van Nieuwkerk and F. H. L. Essler, On the low-energy description for tunnel-coupled one-dimensional Bose gases, SciPost Phys. **9**, 025 (2020).

[52] J.-F. Mennemann, I. E. Mazets, M. Pigneur, H. P. Stimming, N. J. Mauser, J. Schmiedmayer, and S. Erne, Relaxation in an extended bosonic Josephson junction, Phys. Rev. Res. **3**, 023197 (2021).

[53] A. Imambekov and L. I. Glazman, Universal theory of nonlinear Luttinger liquids, Science **323**, 228 (2009).

[54] A. Steffens, M. Friesdorf, T. Langen, B. Rauer, T. Schweigler, R. Hübener, J. Schmiedmayer, C. Riofrío, and J. Eisert, Towards experimental quantum-field tomography with ultracold atoms, Nat. Commun. **6**, 7663 (2015).

[55] M. Aidelsburger, J. L. Ville, R. Saint-Jalm, S. Nascimbène, J. Dalibard, and J. Beugnon, Relaxation dynamics in the merging of $n$ independent condensates, Phys. Rev. Lett. **119**, 190403 (2017).

[56] S. Sunami, V. P. Singh, D. Garrick, A. Beregi, A. J. Barker, K. Luksch, E. Bentine, L. Mathey, and C. J. Foot, Observation of the Berezinskii-Kosterlitz-Thouless transition in a two-dimensional Bose gas via matter-wave interferometry, Phys. Rev. Lett. **128**, 250402 (2022).

[57] S. Sunami, V. P. Singh, D. Garrick, A. Beregi, A. J. Barker, K. Luksch, E. Bentine, L. Mathey, and C. J. Foot, Universal scaling of the dynamic BKT transition in quenched 2D Bose gases, Science **382**, 443 (2023).

[58] S. Sunami, V. P. Singh, E. Rydow, A. Beregi, E. Chang, L. Mathey, and C. J. Foot, Detecting phase coherence of 2D Bose gases via noise correlations, arXiv:2406.03491.

[59] Y. Nakamura, Y. Takasu, J. Kobayashi, H. Asaka, Y. Fukushima, K. Inaba, M. Yamashita, and Y. Takahashi, Experimental determination of Bose-Hubbard energies, Phys. Rev. A **99**, 033609 (2019).

[60] M. Atala, M. Aidelsburger, M. Lohse, J. T. Barreiro, B. Paredes, and I. Bloch, Observation of chiral currents with ultracold atoms in bosonic ladders, Nat. Phys. **10**, 588 (2014).

[61] T. Langen, T. Schweigler, E. Demler, and J. Schmiedmayer, Double light-cone dynamics establish thermal states in integrable 1D Bose gases, New J. Phys. **20**, 023034 (2018).